AMERICAN SOCIETY FOR MICROBIOLOGY | Infection and Immunity®

HOST RESPONSE AND INFLAMMATION

Interleukin-22 (IL-22) Binding Protein Constrains IL-22 Activity, Host Defense, and Oxidative Phosphorylation Genes during Pneumococcal Pneumonia

Giraldina Trevejo-Nunez,[a] Waleed Elsegeiny,[b] Felix E. Y. Aggor,[c] Jamie L. Tweedle,[c] Zoe Kaplan,[b] Pranali Gandhi,[c] Patricia Castillo,[b] Annabel Ferguson,[d] John F. Alcorn,[b] Kong Chen,[d] Jay K. Kolls,[b,e] Sarah L. Gaffen[c]

[a]Division of Infectious Diseases. University of Pittsburgh School of Medicine, Pittsburgh, Pennsylvania, USA
[b]UPMC Children's Hospital of Pittsburgh, Pittsburgh, Pennsylvania, USA
[c]Division of Rheumatology and Clinical Immunology, University of Pittsburgh School of Medicine, Pittsburgh, Pennsylvania, USA
[d]Division of Pulmonary, Allergy and Critical Care Medicine, University of Pittsburgh School of Medicine, Pittsburgh, Pennsylvania, USA
[e]Tulane University School of Medicine, New Orleans, Louisiana, USA

ABSTRACT *Streptococcus pneumoniae* is the most common cause of community-acquired pneumonia worldwide, and interleukin-22 (IL-22) helps contain pneumococcal burden in lungs and extrapulmonary tissues. Administration of IL-22 increases hepatic complement 3 and complement deposition on bacteria and improves phagocytosis by neutrophils. The effects of IL-22 can be tempered by a secreted natural antagonist, known as IL-22 binding protein (IL-22BP), encoded by *Il22ra2*. To date, the degree to which IL-22BP controls IL-22 in pulmonary infection is not well defined. Here, we show that *Il22ra2* inhibits IL-22 during *S. pneumoniae* lung infection and that *Il22ra2* deficiency favors downregulation of oxidative phosphorylation (OXPHOS) genes in an IL-22-dependent manner. *Il22ra2*$^{-/-}$ mice are more resistant to *S. pneumoniae* infection, have increased IL-22 in lung tissues, and sustain longer survival upon infection than control mice. Transcriptome sequencing (RNA-seq) analysis of infected *Il22ra2*$^{-/-}$ mouse lungs revealed downregulation of genes involved in OXPHOS. Downregulation of this metabolic process is necessary for increased glycolysis, a crucial step for transitioning to a proinflammatory phenotype, in particular macrophages and dendritic cells (DCs). Accordingly, we saw that macrophages from *Il22ra2*$^{-/-}$ mice displayed reduced OXPHOS gene expression upon infection with *S. pneumoniae*, changes that were IL-22 dependent. Furthermore, we showed that macrophages express IL-22 receptor subunit alpha-1 (IL-22Ra1) during pneumococcal infection and that *Il22ra2*$^{-/-}$ macrophages rely more on the glycolytic pathway than wild-type (WT) controls. Together, these data indicate that IL-22BP deficiency enhances IL-22 signaling in the lung, thus contributing to resistance to pneumococcal pneumonia by downregulating OXPHOS genes and increasing glycolysis in macrophages.

KEYWORDS IL-22BP, OXPHOS, host defense

Streptococcus pneumoniae (pneumococcus) is the leading bacterial pathogen responsible for community-acquired pneumonia (CAP), accounting for 9% of CAP cases (1). Pneumococcus is a major determinant of hospital intensive care unit (ICU) admissions due to severe pneumonia (2) and causes significant morbidity and mortality in critically ill patients (3). We previously reported that treatment with exogenous recombinant interleukin-22 (IL-22) in a mouse model of pneumococcal pneumonia decreased bacterial burdens in lung and extrapulmonary organs (4). In this model, administration of recombinant IL-22 improved complement 3 (C3) deposition on pneumococci, thereby improving bacterial phagocytosis by neutrophils.

Citation Trevejo-Nunez G, Elsegeiny W, Aggor FEY, Tweedle JL, Kaplan Z, Gandhi P, Castillo P, Ferguson A, Alcorn JF, Chen K, Kolls JK, Gaffen SL. 2019. Interleukin-22 (IL-22) binding protein constrains IL-22 activity, host defense, and oxidative phosphorylation genes during pneumococcal pneumonia. Infect Immun 87:e00550-19. https://doi.org/10.1128/IAI.00550-19.

Editor Nancy E. Freitag, University of Illinois at Chicago

Copyright © 2019 American Society for Microbiology. All Rights Reserved.

Address correspondence to Giraldina Trevejo-Nunez, giraldina.trevejo@pitt.edu.

Received 18 July 2019
Returned for modification 3 August 2019
Accepted 15 August 2019
Accepted manuscript posted online 26 August 2019
Published 18 October 2019

Downloaded from https://journals.asm.org/journal/iai on 06 February 2025 by 18.97.14.90.

IL-22, which is produced mainly by lymphoid lineage cells (NK cells, T cells, innate lymphoid cells [ILCs], and γδ T cells), signals through a dimeric receptor composed of IL-22 receptor subunit alpha-1 (IL-22Ra1) and IL-10R2. IL-22Ra1 is localized at epithelial surface barriers, including the lung epithelial surface (5). On the other hand, IL-22 signaling is negatively regulated by a soluble decoy receptor, called the interleukin 22 binding protein (IL-22BP), also known as IL-22Ra2. Expression of IL-22BP is abundant in lymph nodes, spleen, lung, thymus (6), intestinal Peyer's patches (7), and colon. Peyer's patches' dendritic cells (DCs), lamina propria DCs, lamina propria macrophages, and $CD4^+$ T cells express the most IL-22BP (7–9). The role of IL-22BP as an endogenous IL-22 inhibitor was first demonstrated *in vitro*. IL-22BP showed 1,000 times greater affinity for IL-22 than the latter for its natural receptor, IL-22Ra1. Subsequent data from *in vivo* models of intestinal infection and inflammation have further supported an inhibitory role for IL-22BP. For instance, during the recovery phase of colonic epithelial regeneration after dextran sulfate sodium (DSS) colitis, IL-22BP deficiency caused IL-22-induced excessive epithelial proliferation and increases in tumor burden (10). Similarly, in a $CD4^+$ T cell transfer colitis model, IL-22BP-deficient, IL-22-sufficient $CD4^+$ $CD45RB^{hi}$ T cells were less pathogenic than wild-type (WT) counterparts when transferred to *Rag1*$^{-/-}$ recipients (9).

The lung also expresses IL-22BP, but surprisingly few studies have reported the significance of IL-22BP deficiency during pneumonia. Here we show that an absence of IL-22BP benefits the host in the context of pneumococcal lung infection. Transcriptome sequencing (RNA-seq) analysis of infected *Il22ra2*$^{-/-}$ mouse lung tissue indicated that the beneficial effects of increased IL-22 in lung tissues, secondary to IL-22BP deficiency, favor downregulation of OXPHOS genes. Increased IL-22 not only signals lung epithelial cells, but also affects pulmonary macrophages, downregulating OXPHOS genes. These changes in OXPHOS genes drive macrophages to a more inflammatory state, resulting in decreased bacterial burdens in the *Il22ra2*$^{-/-}$ mice.

RESULTS

$CD45^-$ lung cells express IL-22BP. To date, little is known about IL-22BP expression in the lungs. Hence, lung cells were sorted by fluorescence-activated cell sorter (FACS). The following groups were subjected to quantitative PCR (qPCR): $CD45^-$ $CD31^+$ $Pdpn^-$, $CD45^-$ $CD31^-$ $Pdpn^-$, $CD45^-$ $CD31^+$ $Pdpn^+$, $CD45^-$ $CD31^-$ $Pdpn^+$, and $CD45^+$. As shown, *Il22ra1* mRNA expression was most abundant in the $CD45^-$ $CD31^-$ $Pdpn^-$ group (Fig. 1A). In contrast, *Il22ra2* mRNA expression (IL-22BP) was highest in the $CD45^-$ $CD31^-$ $Pdpn^+$ and $CD45^-$ $CD31^-$ $Pdpn^-$ groups (Fig. 1B). To validate the identity of the $CD45^-$ populations, we tested lung-cell-specific genes: genes coding for aquaporin 5 (*Aqp5*), surfactant protein C (*Sftpc*), Clara cell secretory protein (*Ccsp*), and forkhead box protein J1 (*Foxj1*). *Aqp5* and *Sftpc* are well described as being expressed by alveolar cells (11) and were indeed highly expressed in the $CD45^-$ $CD31^-$ $Pdpn^+$ group. *Ccsp* and *Foxj1* are known to be highly expressed in bronchial epithelial cells and consistently also had high expression in the $CD45^-$ $CD31^-$ $Pdpn^-$ group (Fig. 1C). Taken together, this information confirms that *Il22ra1* is more abundant in bronchial epithelial cells (12) and suggests that *Il22ra2* is expressed in alveolar cells.

IL-22BP-deficient mice are more resistant to pneumococcal lung infection than WT mice. In the course of the above analyses, we noticed that uninfected *Il22ra2*$^{-/-}$ mice have higher levels of serum IL-22 than uninfected WT mice (Fig. 2A). Accordingly, we postulated that *Il22ra2*$^{-/-}$ mice might show resistance to pneumococcal pneumonia. To test this hypothesis, *Il22ra2*$^{-/-}$ mice and WT controls were infected with pneumococcus by oropharyngeal aspiration. After 48 h, lung bacterial burdens in *Il22ra2*$^{-/-}$ and WT mice were assessed by CFU enumeration. As shown, *Il22ra2*$^{-/-}$ lung burdens were lower than those of WT controls (Fig. 2B). The decrease in burden was not seen in the spleen (Fig. 2C), suggesting that the protective phenotype in the absence of IL-22BP is local to the site of infection. *Il22ra2*$^{-/-}$ mice also displayed increased levels of IL-22-dependent genes, such as *Lyz1*, *Saa1*, and *Il36g* (Fig. 2D). These correlated with increased IL-22 protein expression in lung tissue at 12 h postinfection (Fig. 2E). Fur-

Downloaded from https://journals.asm.org/journal/iai on 06 February 2025 by 18.97.14.90.

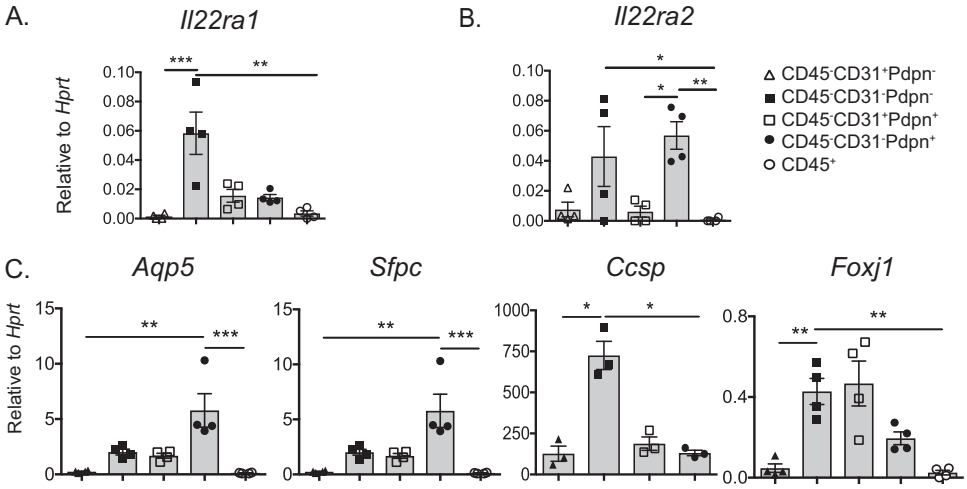

FIG 1 CD45$^-$ lung cells express IL-22BP. Naïve lung cells from WT mice were sorted and classified into CD45$^-$ CD31$^+$ Pdpn$^-$, CD45$^-$ CD31$^-$ Pdpn$^-$, CD45$^-$ CD31$^+$ Pdpn$^+$, CD45$^-$ CD31$^-$ Pdpn$^+$, and CD45$^+$ populations and subjected to qPCR. Gene expression is normalized to *Hprt*. Genes: (A) *Il22ra1*, (B) *Il22ra2*, (C) *Aqp5* (aquaporin 5), *Sftpc* (surfactant protein C), *Ccsp* (Clara cell secretory protein), and *Foxj1* (forkhead box J1). *, $P < 0.05$; **, $P < 0.01$; ***, $P < 0.001$ (Kruskal-Wallis test). Data are representative of two experiments.

thermore, *Il22ra2*$^{-/-}$ mice survived longer than WT controls when infected with pneumococcus (Fig. 2F). In bronchoalveolar lavage (BAL) fluid, there was similar protein expression of cytokines (gamma interferon [IFN-γ], tumor necrosis factor alpha [TNF-α], IL-6, IL-1β, and IL-17) and chemokines (CXCL1, CXCL2, and CXCL5) (see Fig. S1A in the supplemental material), as well as cellular recruitment of macrophages and neutrophils to lung (Fig. S1B). Increased levels of IL-22 did not correlate with higher expression of tight junction genes or decrease in lung permeability (Fig. S1C). These findings suggest that IL-22BP deficiency allows for enhanced endogenous IL-22 activity.

IL-22BP deficiency impairs OXPHOS gene expression during pneumococcal lung infection. To determine how IL-22BP deficiency causes resistance to pneumococcal pneumonia, WT and *Il22ra2*$^{-/-}$ mice were infected with pneumococcus and lung tissue was subjected to RNA-seq. A total of 1,215 genes were differentially expressed in the WT and *Il22ra2*$^{-/-}$ groups ($P < 0.05$). Of these, 409 were differentially expressed only in the *Il22ra2*$^{-/-}$ mice. Analysis by the Ingenuity Pathway Analysis (IPA) program revealed several pathways that are implicated in cellular metabolic function. These include mitochondrial dysfunction, oxidative phosphorylation (OXPHOS), the sirtuin signaling pathway, STAT3 pathway, and the pentose phosphate pathway (Fig. 3A). We were particularly struck by the finding of the OXPHOS pathway in this setting. Impairment of mitochondrial OXPHOS is necessary for optimal immune cell activation—especially for M1 macrophage polarization (13, 14) and DC activation (15, 16). Accordingly, 24 genes were downregulated in the OXPHOS pathway in the *Il22ra2*$^{-/-}$ group compared to the WT (Fig. 3B). Hence, the IL-22/IL-22BP axis appears to modulate OXPHOS genes during pneumococcal infection.

Control of OXPHOS genes is IL-22 dependent. During bacterial pneumonia, immune cells in the lung represent 70% of the total cells. In order to understand which immune population is responsible for the OXPHOS gene differences seen in the RNA-seq analysis, we FACS sorted CD45$^+$ CD11c^{hi} F4/80$^+$ (macrophages), CD45$^+$ CD11c^{hi} F4/80$^-$ (DCs), and CD45$^+$ Ly6G$^+$ (neutrophils) cells and subjected each group to qPCR of representative OXPHOS genes. Results from CD45$^+$ CD11c^{hi} F4/80$^+$ (macrophages) and CD45$^+$ CD11c^{hi} F4/80$^-$ (DCs) cells mirrored the findings of OXPHOS gene changes in RNA-seq (see Fig. S2 in the supplemental material). To determine if the downregulation of OXPHOS genes in the *Il22ra2*$^{-/-}$ group was in fact IL-22 dependent, CD11c$^+$ cells were sorted from WT, *Il22ra2*$^{-/-}$, *Il22*$^{-/-}$, and double knockout (DKO) *Il22ra2*$^{-/-}$ *Il22*$^{-/-}$ lungs. As shown, a deficiency in IL-22 correlated with increased

Downloaded from https://journals.asm.org/journal/iai on 06 February 2025 by 18.97.14.90.

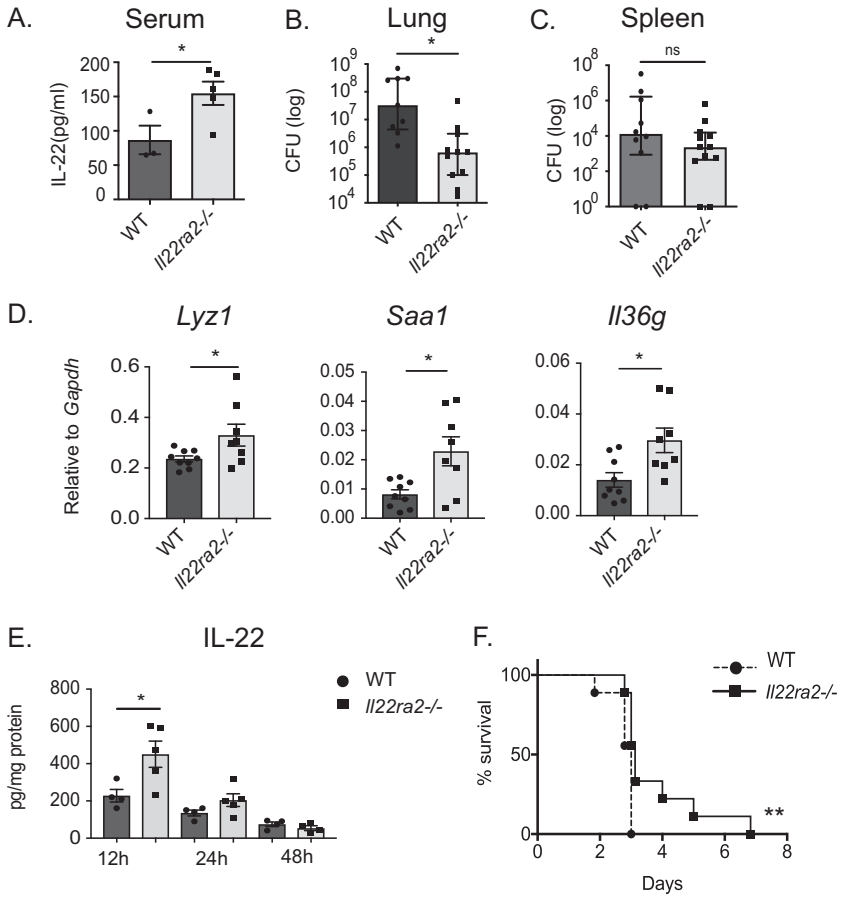

FIG 2 *Il22ra2*$^{-/-}$ mice show increased resistance to pneumococcal lung infection. (A) IL-22 in serum of uninfected mice was measured by ELISA. (B) Lung and (C) spleen bacterial burden in WT and *Il22ra2*$^{-/-}$ mice at 48 h postinfection. (D) Gene expression of *Saa1*, *Lyz1*, and *Il36g* in lung tissue of WT and *Il22ra2*$^{-/-}$ mice was assessed by qPCR at 12 h postinfection. (E) IL-22 protein in lung tissue homogenate at 12, 24, and 48 h postinfection was measured by ELISA. Data in panels A, D, and E are mean ± SEM. Data in panels B and C are the median with interquartile range. *, $P < 0.05$ (two-tailed Mann-Whitney test); ns, not significant. (F) Survival of WT and *Il22ra2*$^{-/-}$ mice following *S. pneumoniae* lung infection. $n = 9$ mice/group. **, $P < 0.01$ (log-rank Mantel-Cox test). Data are representative of two experiments.

expression of OXPHOS genes, while the absence of the decoy receptor IL-22BP correlated with decreased expression of OXPHOS genes (Fig. 4A). For most of the genes tested, a lack of both IL-22 and IL-22BP correlated with an increase in OXPHOS genes. Overall, these data confirm that pneumococcal pneumonia induces changes in OXPHOS genes and that such changes are IL-22 dependent. Moreover, these data verify that IL-22BP is a bona fide antagonist of IL-22 *in vivo*.

IL-22 signals lung epithelial cells and macrophages. Since the IL-22 receptor (IL-22Ra1) is present in bronchial epithelial cells (5), we assessed signaling in MLE-12 cells, an immortalized distal respiratory epithelial cell line that is a surrogate for lung epithelial cells. To assess IL-22Ra1 functionality, cells were stimulated with IL-22 and phosphorylation of STAT3 was assessed by immunoblotting (Fig. 4B) over a time course of 15, 30, and 60 min. As shown, IL-22 activated STAT3 at 60 min. We also reasoned that the IL-22-dependent effects in OXPHOS genes would likely occur in the lung epithelium. Stimulation of MLE-12 cells with IL-22 indeed induced downregulation in OXPHOS genes (Fig. 4C).

In our study, sorted macrophages (CD45$^+$ CD11c^{hi} F4/80$^+$) are the main group of cells that display downregulation of OXPHOS genes (Fig. S2). This downregulation is more pronounced in *Il22ra2*$^{-/-}$ mice, in which IL-22 is more abundant. Hence, we postulated that IL-22 signals directly in macrophages during pneumococcal pneumo-

Downloaded from https://journals.asm.org/journal/iai on 06 February 2025 by 18.97.14.90.

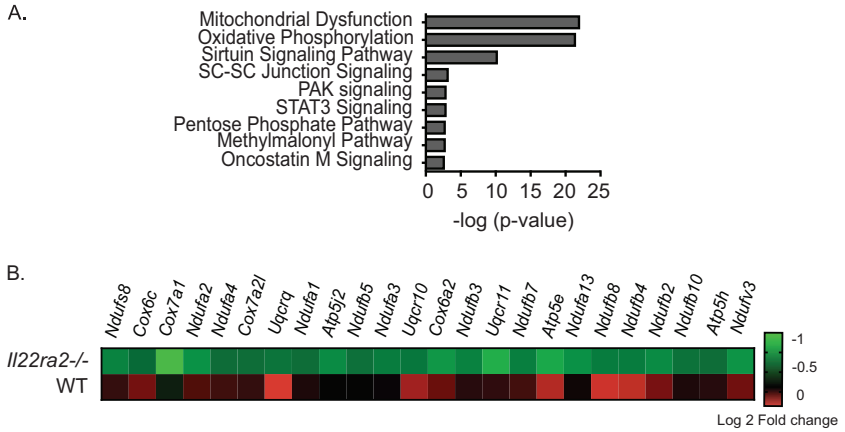

FIG 3 IL-22BP alters OXPHOS gene expression during pneumococcal lung infection. WT and *Il22ra2*$^{-/-}$ mice were infected with *S. pneumoniae* for 12 h. RNA from total lung tissues of naive and infected mice was subjected to RNA-seq. (A) Ingenuity Pathway Analysis of differentially expressed genes in the *Il22ra2*$^{-/-}$ mice compared to the WT. (B) Heat map of genes involved in the OXPHOS pathway. $n = 2$/group.

nia. To address this question, we first stained for IL-22Ra1 in infected lungs of WT and *Il22ra2*$^{-/-}$ mice. As shown by immunofluorescence (IF) and immunohistochemistry (IHC), IL-22Ra1 was detected not only in bronchial epithelium but also in macrophages of WT and *Il22ra2*$^{-/-}$ lungs (Fig. 5A). IL-22Ra1 is expressed in foamy cells, which have the morphology of macrophages (Fig. 5C). Lysozyme, a marker of myeloid cells, costained with IL-22Ra1 (Fig. 5B), confirming macrophage-specific staining of this receptor.

To determine IL-22 signaling in macrophages, we differentiated bone marrow-derived macrophages (BMDMs) and assessed STAT3 phosphorylation. BMDMs showed phosphorylation of STAT3 as early as 15 min (see Fig. S3A in the supplemental material). Furthermore, *Il22ra2*$^{-/-}$ BMDMs stimulated with IL-22 had increased downregulation of OXPHOS genes compared to WT BMDMs as early as 2 h poststimulation (Fig. S3B). These experiments show that IL-22 not only signals through the lung epithelium but also signals to macrophages during pneumococcal pneumonia. Thus, we conclude that macrophages have the capacity to express IL-22R during pneumococcal pneumonia and respond by activating STAT3.

IL-22BP-deficient macrophages are more glycolytic than WT macrophages. Once macrophages become proinflammatory, these cells favor glycolysis while OXPHOS is suppressed. To evaluate if the downregulation of OXPHOS genes between WT and *Il22ra2*$^{-/-}$ macrophages represented OXPHOS suppression in favor of glycolysis, we performed functional analysis of mitochondria. To ensure that changes in mitochondrial respiration were not merely due to differences in mitochondrial quantity, we evaluated mitochondrial mass by flow cytometry using MitoTracker Green FM, a membrane-permeable fluorescent dye used to stain mitochondrial mass (17). As shown, mitochondrial masses were indeed similar between WT and *Il22ra*$^{-/-}$ macrophages at baseline and during infection (Fig. 6A). We also assessed mitochondrial transmembrane potential, a gradient of electrical polarization in the inner mitochondrial membrane that reflects electron transport. This parameter was evaluated by flow cytometry using tetramethylrhodamine ester (TMRE). As depicted, mitochondrial potential was increased to a similar degree between infected WT and *Il22ra2*$^{-/-}$ macrophages upon infection (Fig. 6B).

The fact that mitochondrial mass and potential were not different between WT and *Il22ra2*$^{-/-}$ macrophages suggested that the mitochondria were not dysfunctional at baseline and could depolarize similarly during infection. Thus, we hypothesized that the functional differences between WT and *Il22ra2*$^{-/-}$ macrophages would likely be in mitochondrial respiration and glycolysis. To assess differences in the metabolic phe-

Downloaded from https://journals.asm.org/journal/iai on 06 February 2025 by 18.97.14.90.

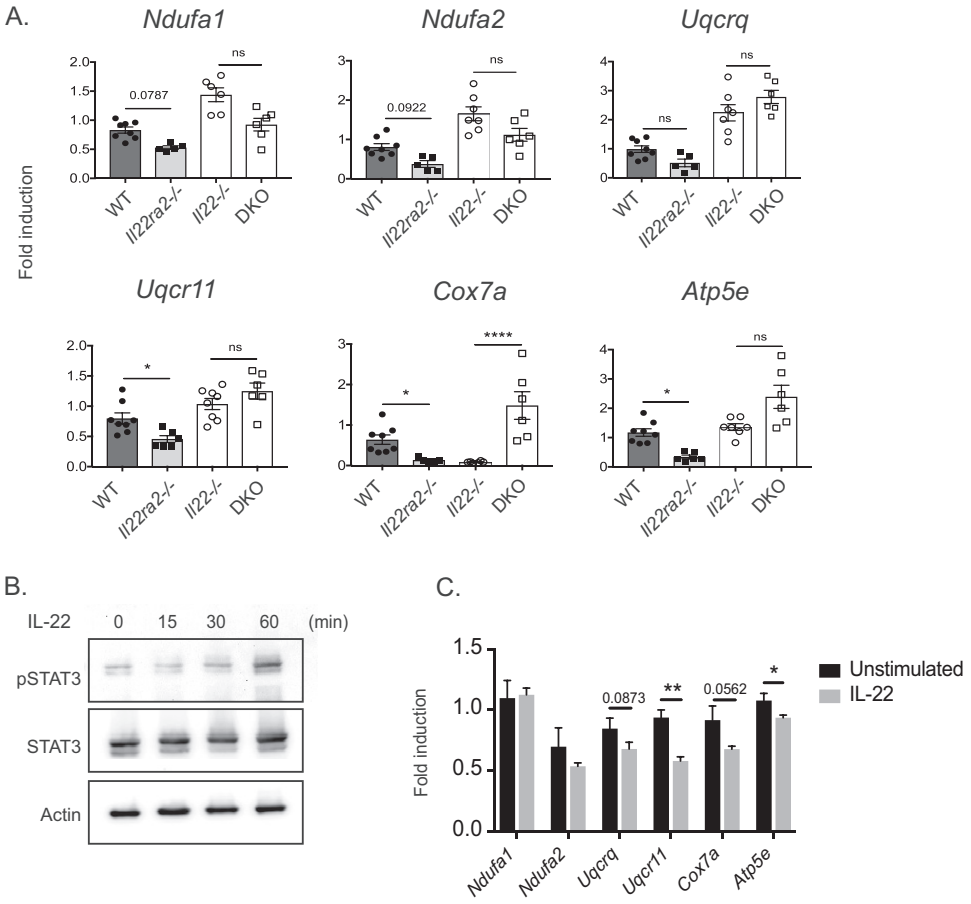

FIG 4 Downregulation of OXPHOS genes is IL-22 dependent. (A) CD11c$^+$ sorted lung cells from WT, *Il22ra2*$^{-/-}$, *Il22*$^{-/-}$, and DKO (*Il22ra2*$^{-/-}$ *Il22*$^{-/-}$) mice were sorted at 12 h postinfection. Expression of OXPHOS genes is represented as fold induction relative to uninfected. Data are mean ± SEM. *, $P < 0.05$; ****, $P < 0.0001$; ns, not significant (Kruskal-Wallis test). Each dot represents one mouse. (B) MLE-12 cells were stimulated with IL-22 (100 ng/ml) at the indicated time points and assessed for pSTAT3 by Western blotting. (C) MLE-12 cells were stimulated with IL-22 for 6 h, and OXPHOS genes were assessed as fold induction relative to those in unstimulated cells. Data are mean ± SEM. *, $P < 0.05$; **, $P < 0.01$ (Mann-Whitney test); ns, not significant. Data are representative of two experiments.

notype, we measured mitochondrial oxygen consumption (oxygen consumption rate [OCR]), using a Seahorse extracellular flux analyzer (Fig. 6C), in WT and *Il22ra*$^{-/-}$ CD11c$^+$ cells sorted from infected and uninfected lungs. Mitochondria were stressed by serial administration of inhibitors of the electron transport chain (ETC): oligomycin, which inhibits complex V; carbonyl cyanide-4 (trifluoromethoxy) phenylhydrazone (FCCP), which uncouples the mitochondrial inner membrane; and a rotenone-antimycin mixture, which impairs complexes I and III, respectively. Then we calculated mitochondrial functional parameters: basal respiration, ATP-linked respiration, maximal respiration, and spare respiratory capacity (Fig. 6D). These parameters were modestly increased in WT compared to *Il22ra2*$^{-/-}$ cells, suggesting that during infection, *Il22ra2*$^{-/-}$ macrophages use less OXPHOS than WT controls as the main source of energy.

Since use of mitochondrial OXPHOS was decreased in *Il22ra2*$^{-/-}$ macrophages, we assessed glycolysis by evaluating uptake of 2-NBDG, a glucose analog and surrogate marker of glycolysis. *Il22ra2*$^{-/-}$ macrophages from infected mice displayed increased 2-NBDG uptake compared to WT macrophages, suggesting that *Il22ra2*$^{-/-}$ macrophages are more glycolytic than the WT ones (Fig. 6E). Overall, these data suggest that *Il22ra2*$^{-/-}$ macrophages rely more on glycolysis than WT macrophages.

Downloaded from https://journals.asm.org/journal/iai on 06 February 2025 by 18.97.14.90.

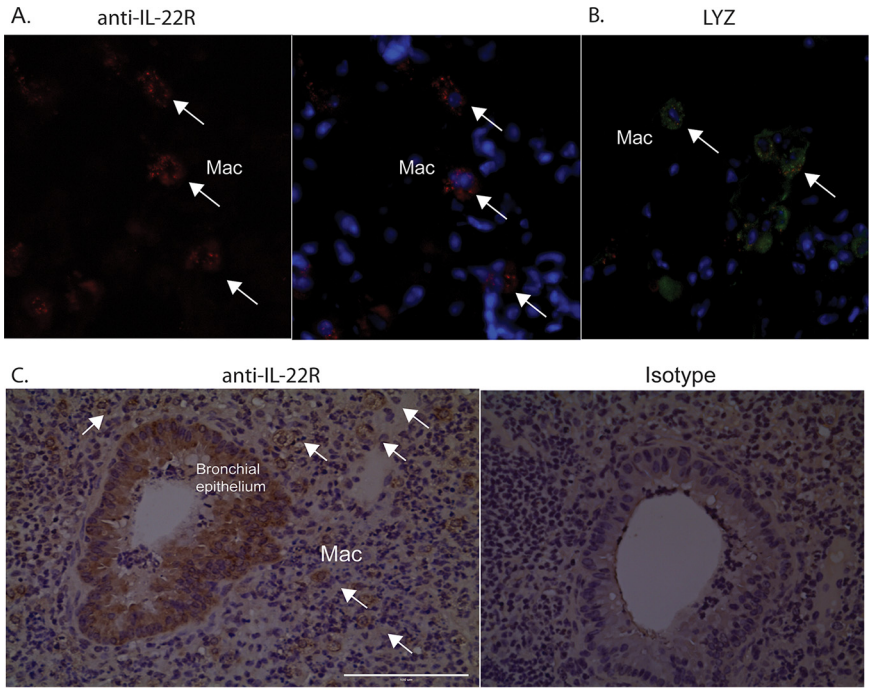

FIG 5 IL-22R is expressed in macrophages and lung epithelial cells. (A and B) Immunofluorescent labeling with (A) anti-IL-22R and (B) antilysozyme (LYZ), a marker of myeloid cells of murine lung sections infected with *S. pneumoniae*. (C) Immunohistochemical labeling of infected lung tissue with anti-IL-22R. Mac, macrophage. White arrows indicate macrophages. Data are representative of two experiments.

DISCUSSION

Animal models of inflammation have mostly been consistent with the idea that IL-22BP negatively regulates IL-22 downstream signaling. Thus, IL-22BP deficiency either benefits or harms the host, depending on the organ affected or the type of inflammation. For example, in a model of $CD4^+$ T cell transfer colitis, donor IL-22BP-deficient $CD4^+$ T cells induced less epithelial damage in *Rag1*$^{-/-}$ recipients, which was secondary to the unrestricted IL-22 epithelial regenerative capacity (9). In a chronic model of DSS colitis, IL-22BP deficiency rendered mice susceptible to increased colon tumor burden, which was attributable to excessive IL-22-induced epithelial proliferation (10). In the liver, absence of IL-22BP was found to be detrimental during acute reperfusion liver injury (18) due to increased IL-22-induced *Cxcl10* expression. Thus, these published data provide evidence that IL-22 is inhibited by IL-22BP *in vivo* during an inflammatory process.

Our findings support all the above data in that IL-22BP is an inhibitor of IL-22 in the lung. We find that IL-22BP deficiency protects the host following *S. pneumoniae* infection by decreasing the infectious burden and prolonging survival upon infection. Host protection correlates with the observation that IL-22BP-deficient mice have increased serum IL-22 at baseline as well as increased IL-22 in lung after infection with pneumococcus.

However, the mechanism by which IL-22 benefits the host appears to be distinct. In line with the host protection mechanisms, IL-22 is typically considered to defend the host by (i) production of antimicrobial peptides (AMPs), (ii) epithelial regeneration, and (iii) increased cellular recruitment to the site of inflammation. These response mechanisms are tissue and pathogen specific. Here, we propose that increased IL-22 due to IL-22BP deficiency downregulates OXPHOS genes in lung epithelial cells and macrophages during pneumococcal infection. Our data show that IL-22BP-deficient mice, which have increased IL-22, do not rely solely on the classic IL-22-mediated mechanisms of host defense. Rather, IL-22 also influences macrophage mitochondrial metabolism. This is supported by the findings of RNA-seq analysis of infected lungs, which

Downloaded from https://journals.asm.org/journal/iai on 06 February 2025 by 18.97.14.90.

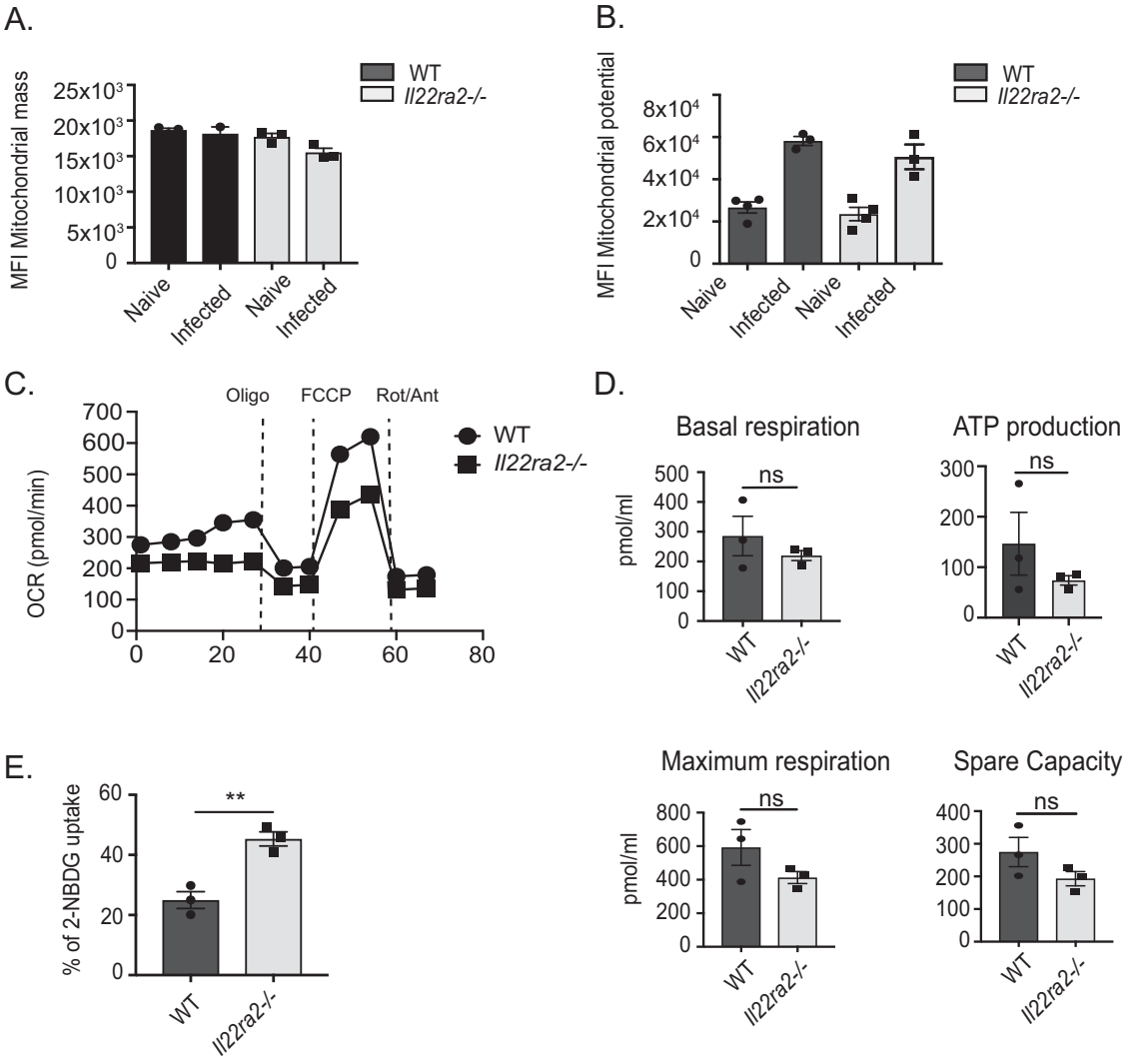

FIG 6 *Il22ra2*$^{-/-}$ macrophages are more glycolytic than WT macrophages. Alveolar macrophages (Cd11c^{hi} F4/80^{+} cells) were assessed by flow cytometry for (A) mitochondrial mass using Mitotracker Green FM and (B) mitochondrial potential using TMRE. MFI, mean fluorescent intensity. (C) CD11c^{+} cells from pneumococcus-infected mice were sorted and evaluated for oxygen consumption rate (OCR) by Seahorse flux analyzer. (D) Basal respiration, ATP production, spare capacity, and maximum respiration were calculated from OCR data. (E) Glycolysis of alveolar macrophages (Cd11c^{hi} F4/80^{+}) was assessed by flow cytometry using 2-NBDG fluorescent dye uptake. Data are mean ± SEM in panels A, B, D, and E. **, $P < 0.05$ (Mann-Whitney test); ns, not significant. Data are representative of two independent experiments.

displayed multiple genes clustered in the OXPHOS pathway that were suppressed in the IL-22BP-deficient compared to WT mice.

Another surprising finding was the observation that IL-22Ra1 signals in macrophages. It is thought that IL-22Ra1 is only expressed at epithelial barriers of mucosal surfaces (19), and in the lung, IL-22Ra1 is present in the bronchial epithelium (5, 12). We reasoned that the bronchial epithelium was the primary site accounting for changes of OXPHOS genes in total lung RNA-seq. However, the expression of these OXPHOS genes was not significantly changed in bronchial brushes from pneumococcus-infected mice (unpublished data). On the contrary, our data indicate that macrophages account for the downregulation of OXPHOS genes observed in total lung RNA-seq. This observation led us to hypothesize that IL-22 signals directly in macrophages. To demonstrate this point, we showed expression of IL-22Ra1 in macrophages of infected lungs and pSTAT3 signaling upon IL-22 stimulation in BMDMs. Our findings are supported by a recent paper showing that IL-22Ra1 is expressed in macrophages that accumulate during chronic stages of infection in the tuberculous granuloma (20). Thus, our data suggest

Downloaded from https://journals.asm.org/journal/iai on 06 February 2025 by 18.97.14.90.

that IL-22Ra1 can indeed be induced during pneumococcal pneumonia in macrophages.

Since IL-22BP-deficient macrophages displayed the most prominent downregulation of OXPHOS genes during pneumococcal infection, we assessed mitochondrial function between WT and *Il22ra2*$^{-/-}$ macrophages *ex vivo*. It is known that these cells change their metabolism from primarily relying on OXPHOS at rest to glycolysis during LPS stimulation (14, 16). Downregulation of OXPHOS during LPS stimulation is mostly secondary to nitric oxide production, which blocks complex I of the ETC, and is also secondary to interruption of the tricarboxylic acid (TCA) cycle. Impaired OXPHOS also induces the shunt pentose phosphate pathway (PPP) (21, 22), which is important for reactive oxygen species (ROS) production and for increases in intermediary products of the interrupted TCA cycle, such as citrate, succinate, and itaconate (13, 23, 24). These by-products of the TCA cycle impact the proinflammatory state of macrophages and DCs, benefiting host resistance against infection.

In this study, we showed that sorted CD11c^{+} cells from infected *Il22ra2*$^{-/-}$ lungs have decreased parameters of mitochondrial respiration compared to the WT (decreased basal respiration, ATP production, and spare respiratory capacity), which suggests that IL-22 in IL-22BP-deficient macrophages contributes to impairment of mitochondrial OXPHOS. This step favors increases in glycolysis during pneumococcal pneumonia.

In summary, this work supports a role of IL-22BP as a natural inhibitor of IL-22 in the lung, favoring IL-22 signaling in macrophages to increase impairment of mitochondrial OXPHOS and improve glycolysis during pneumococcal pneumonia.

MATERIALS AND METHODS

Mice. *Il22ra2*$^{-/-}$ mice (C57BL/6 background) were a gift from Genentech. *Il22ra2*$^{+/+}$ (WT) controls and *Il22ra*$^{-/-}$ mice were used for all experiments. All mice were 8 to 10 weeks old, and both male and female mice were used. All animal studies were approved by the Institutional Animal Care and Use Committee of the University of Pittsburgh. *Il22*$^{-/-}$ mice were obtained from Taconic Biosciences.

Pneumococcus infections. *Streptococcus pneumoniae* serotype 3 (ATCC 6303) was grown in Todd-Hewitt broth (4), and 10^6 CFU/mouse was given by oropharyngeal aspiration in 50 μl phosphate-buffered saline (PBS). For survival studies, 10^4 CFU/mouse was given by oropharyngeal aspiration. Mice were monitored twice a day for signs of distress and weighed daily.

Bacterial burden, mRNA, and protein analysis. Tissues were homogenized in PBS, and CFU were assessed by plating in serial dilutions. Lungs were homogenized in TRIzol (Invitrogen). One microgram of RNA was used to synthesize cDNA. Primers with SSOFast Probes Supermix probes were used for qPCR. Threshold cycle (C_T) values were normalized to *Hprt* or *Gapdh*. For IL-22 protein detection, lung homogenates were assessed by enzyme-linked immunosorbent assay (ELISA) (Invitrogen).

Flow cytometry. Lungs were digested with collagenase D (2 mg/ml), and red blood cells (RBCs) were lysed with ammonium chloride. Single-cell suspensions were stained with CD16/32 (eBioscience). For sorting of pulmonary cell populations, the following antibodies were used: anti-CD45 conjugated with fluorescein isothiocyanate (FITC) (eBioscience; FITC, 11-0454-81; and e450, 48-0454-80, clone 104), anti-CD31 conjugated with allophycocyanin (APC) (eBioscience, 17-0311-80, clone 360), and antipodoplanin conjugated with phycoerythrin (PE) (eBioscience 12-5381-80, clone 8.1.1). Cells were sorted using a FACSAriaII into TRIzol, and RNA was isolated as described above. Ultrapure CD11c^{+} microbeads were used to isolate CD11c^{+} cells (Miltenyi Biotech).

MLE-12 cell culture and stimulation. MLE-12 cells (CRL-2110; ATCC) were grown in HITES medium (Dulbecco's modified Eagle's medium [DMEM] F-12, insulin 0.005 mg/ml, transferrin 0.01 mg/ml, sodium selenite 30 nM, hydrocortisone 10 nM, beta-estradiol 10 nM, L-glutamine 2 mM). Cells were stimulated with IL-22 (100 ng/ml; Peprotech).

RNA-seq. Total RNA was isolated from lung with the Qiagen RNAeasy Plus kit. RNA quality was assessed with the Agilent RNA TapeStation. Libraries were prepared from 500 ng total RNA using the Illumina TruSeq stranded RNA kit. Library quality and concentration were determined with the Agilent DNA TapeStation and qubit fluorometer, respectively. Libraries were sequenced at 1.8 pM on an Illumina NextSeq500 with single 75-bp reads, to a depth of at least 25 million reads. The resulting fastq files were uploaded to the Maverix platform for reading alignment, quantification, and differential gene expression analysis.

Immunohistochemistry and immunofluorescence staining. For IHC, lung sections were deparaffinized in xylene and rehydrated through sequential washings. After antigen retrieval with citrate buffer (10 mM) and peroxidase blocking, slides were blocked using the Vectastain ABC blocking protocol for rat IgG (Vector Laboratories). IL-22Ra1 was visualized using rat anti-mouse IL-22Ra1 (clone 496514; R&D Systems) at a dilution of 1:100. For IF, lung sections were washed with PBS and fixed with 4% paraformaldehyde, followed by permeabilization with 0.25% Triton X-100 in PBS and incubation with rat

Downloaded from https://journals.asm.org/journal/iai on 06 February 2025 by 18.97.14.90.

anti-mouse IL-22Ra1 (1:100) (R&D Systems) and antilysozyme at a dilution of 1:400 (Invitrogen) overnight. Images were captured using the EVOS FL autoimaging system.

Mitochondrial studies. To assess mitochondrial mass, lung cells were stained with Mitotracker Green FM (Invitrogen) (25). To assess mitochondrial potential, cells were stained with tetramethylrhodamine ester (TMRE; Life Tech) and processed as described previously (26). To evaluate glucose uptake, 100 μl of 5 mM 2-NBDG (Cayman Chemical) was administered by tail vein injection. After 30 min, lungs were digested and evaluated by flow cytometry. To measure the oxygen consumption rate (OCR), $CD11c^+$ cells were treated with 1 μM oligomycin, 1.5 μM FCCP (carbonyl cyanide-4 (trifluoromethoxy) phenylhydrazone), and 0.1 μM rotenone plus 1 μM antimycin A using the XFe-96 extracellular flux assay system (Seahorse Biosciences). Seahorse assays were performed in unbuffered DMEM supplemented with 2.5 μM glucose, 1 μM pyruvate, and 2 μM glutamine.

Statistical analyses. An unpaired, two-tailed Mann-Whitney test was used to compare two groups. The Kruskal-Wallis test was used to compare multiple means. All data are displayed as mean ± standard error of the mean (SEM), except for CFU (log-scale) data, which are displayed as median with interquartile range. Significance is indicated as $P < 0.05$.

SUPPLEMENTAL MATERIAL

Supplemental material for this article may be found at https://doi.org/10.1128/IAI.00550-19.

SUPPLEMENTAL FILE 1, PDF file, 0.6 MB.

ACKNOWLEDGMENTS

This work was supported by NHLBI grants R37-HL079142-11S1 (to J.K.K.) and K01-HL135476-02 (to G.T.-N.) and NIDCR grant R37-DE022550 (to S.L.G.).

We thank Akash Verma for insightful comments on the manuscript and Bianca Coleman for technical support. We thank Genentech for *Il22ra2*$^{-/-}$ mice and the Center for Metabolism and Mitochondrial Medicine Bioenergetics Core, University of Pittsburgh, for assisting in mitochondrial metabolic studies.

REFERENCES

1. Musher DM, Abers MS, Bartlett JG. 2017. Evolving understanding of the causes of pneumonia in adults, with special attention to the role of pneumococcus. Clin Infect Dis 65:1736–1744. https://doi.org/10.1093/cid/cix549.
2. Jain S, Self WH, Wunderink RG, Fakhran S, Balk R, Bramley AM, Reed C, Grijalva CG, Anderson EJ, Courtney DM, Chappell JD, Qi C, Hart EM, Carroll F, Trabue C, Donnelly HK, Williams DJ, Zhu Y, Arnold SR, Ampofo K, Waterer GW, Levine M, Lindstrom S, Winchell JM, Katz JM, Erdman D, Schneider E, Hicks LA, McCullers JA, Pavia AT, Edwards KM, Finelli L, CDC EPIC Study Team. 2015. Community-acquired pneumonia requiring hospitalization among U.S. adults. N Engl J Med 373:415–427. https://doi.org/10.1056/NEJMoa1500245.
3. Bedos J-P, Varon E, Porcher R, Asfar P, Le Tulzo Y, Megarbane B, Mathonnet A, Dugard A, Veinstein A, Ouchenir K, Siami S, Reignier J, Galbois A, Cousson J, Preau S, Baldesi O, Rigaud J-P, Souweine B, Misset B, Jacobs F, Dewavrin F, Mira J-P 2018. Host-pathogen interactions and prognosis of critically ill immunocompetent patients with pneumococcal pneumonia: the nationwide prospective observational STREPTOGENE study. Intensive Care Med 44:2162–2173. https://doi.org/10.1007/s00134-018-5444-x.
4. Trevejo-Nunez G, Elsegeiny W, Conboy P, Chen K, Kolls JK. 2016. Critical role of IL-22/IL22-RA1 signaling in pneumococcal pneumonia. J Immunol 197:1877–1883. https://doi.org/10.4049/jimmunol.1600528.
5. Pociask DA, Scheller EV, Mandalapu S, McHugh KJ, Enelow RI, Fattman CL, Kolls JK, Alcorn JF. 2013. IL-22 is essential for lung epithelial repair following influenza infection. Am J Pathol 182:1286–1296. https://doi.org/10.1016/j.ajpath.2012.12.007.
6. Weiss B, Wolk K, Grünberg BH, Volk HD, Sterry W, Asadullah K, Sabat R. 2004. Cloning of murine IL-22 receptor alpha 2 and comparison with its human counterpart. Genes Immun 5:330–336. https://doi.org/10.1038/sj.gene.6364104.
7. Jinnohara T, Kanaya T, Hase K, Sakakibara S, Kato T, Tachibana N, Sasaki T, Hashimoto Y, Sato T, Watarai H, Kunisawa J, Shibata N, Williams IR, Kiyono H, Ohno H. 2017. IL-22BP dictates characteristics of Peyer's patch follicle-associated epithelium for antigen uptake. J Exp Med 214:1607–1618. https://doi.org/10.1084/jem.20160770.
8. Martin JC, Bériou G, Heslan M, Chauvin C, Utriainen L, Aumeunier A, Scott CL, Mowat A, Cerovic V, Houston SA, Leboeuf M, Hubert FX, Hémont C, Merad M, Milling S, Josien R. 2014. Interleukin-22 binding protein (IL-22BP) is constitutively expressed by a subset of conventional dendritic cells and is strongly induced by retinoic acid. Mucosal Immunol 7:101–113. https://doi.org/10.1038/mi.2013.28.
9. Pelczar P, Witkowski M, Perez LG, Kempski J, Hammel AG, Brockmann L, Kleinschmidt D, Wende S, Haueis C, Bedke T, Witkowski M, Krasemann S, Steurer S, Booth CJ, Busch P, König A, Rauch U, Benten D, Izbicki JR, Rösch T, Lohse AW, Strowig T, Gagliani N, Flavell RA, Huber S. 2016. A pathogenic role for T cell-derived IL-22BP in inflammatory bowel disease. Science 354:358–362. https://doi.org/10.1126/science.aah5903.
10. Huber S, Gagliani N, Zenewicz LA, Huber FJ, Bosurgi L, Hu B, Hedl M, Zhang W, O'Connor W, Murphy AJ, Valenzuela DM, Yancopoulos GD, Booth CJ, Cho JH, Ouyang W, Abraham C, Flavell RA. 2012. IL-22BP is regulated by the inflammasome and modulates tumorigenesis in the intestine. Nature 491:259–263. https://doi.org/10.1038/nature11535.
11. Flodby P, Borok Z, Banfalvi A, Zhou B, Gao D, Minoo P, Ann DK, Morrisey EE, Crandall ED. 2010. Directed expression of Cre in alveolar epithelial type 1 cells. Am J Respir Cell Mol Biol 43:173–178. https://doi.org/10.1165/rcmb.2009-0226OC.
12. Aujla SJ, Chan YR, Zheng M, Fei M, Askew DJ, Pociask DA, Reinhart TA, McAllister F, Edeal J, Gaus K, Husain S, Kreindler JL, Dubin PJ, Pilewski JM, Myerburg MM, Mason CA, Iwakura Y, Kolls JK. 2008. IL-22 mediates mucosal host defense against Gram-negative bacterial pneumonia. Nat Med 14:275–281. https://doi.org/10.1038/nm1710.
13. Mills EL, Kelly B, Logan A, Costa ASH, Varma M, Bryant CE, Tourlomousis P, Däbritz JHM, Gottlieb E, Latorre I, Corr SC, McManus G, Ryan D, Jacobs HT, Szibor M, Xavier RJ, Braun T, Frezza C, Murphy MP, O'Neill LA. 2016. Succinate dehydrogenase supports metabolic repurposing of mitochondria to drive inflammatory macrophages. Cell 167:457–470.e13. https://doi.org/10.1016/j.cell.2016.08.064.
14. Jha AK, Huang S-C, Sergushichev A, Lampropoulou V, Ivanova Y, Loginicheva E, Chmielewski K, Stewart KM, Ashall J, Everts B, Pearce EJ, Driggers EM, Artyomov MN. 2015. Network integration of parallel metabolic and transcriptional data reveals metabolic modules that regulate macrophage polarization. Immunity 42:419–430. https://doi.org/10.1016/j.immuni.2015.02.005.

Downloaded from https://journals.asm.org/journal/iai on 06 February 2025 by 18.97.14.90.

15. Everts B, Amiel E, van der Windt GJW, Freitas TC, Chott R, Yarasheski KE, Pearce EL, Pearce EJ. 2012. Commitment to glycolysis sustains survival of NO-producing inflammatory dendritic cells. Blood 120:1422–1431. https://doi.org/10.1182/blood-2012-03-419747.
16. Everts B, Amiel E, Huang S-C, Smith AM, Chang C-H, Lam WY, Redmann V, Freitas TC, Blagih J, van der Windt GJW, Artyomov MN, Jones RG, Pearce EL, Pearce EJ. 2014. TLR-driven early glycolytic reprogramming via the kinases TBK1-IKKε supports the anabolic demands of dendritic cell activation. Nat Immunol 15:323–332. https://doi.org/10.1038/ni.2833.
17. Cottet-Rousselle C, Ronot X, Leverve X, Mayol J-F. 2011. Cytometric assessment of mitochondria using fluorescent probes. Cytometry A 79:405–425. https://doi.org/10.1002/cyto.a.21061.
18. Kleinschmidt D, Giannou AD, McGee HM, Kempski J, Steglich B, Huber FJ, Ernst TM, Shiri AM, Wegscheid C, Tasika E, Hübener P, Huber P, Bedke T, Steffens N, Agalioti T, Fuchs T, Noll J, Lotter H, Tiegs G, Lohse AW, Axelrod JH, Galun E, Flavell RA, Gagliani N, Huber S. 2017. A protective function of IL-22BP in ischemia reperfusion and acetaminophen-induced liver injury. J Immunol 199:4078–4090. https://doi.org/10.4049/jimmunol.1700587.
19. Zheng Y, Valdez PA, Danilenko DM, Hu Y, Sa SM, Gong Q, Abbas AR, Modrusan Z, Ghilardi N, de Sauvage FJ, Ouyang W. 2008. Interleukin-22 mediates early host defense against attaching and effacing bacterial pathogens. Nat Med 14:282–289. https://doi.org/10.1038/nm1720.
20. Treerat P, Prince O, Cruz-Lagunas A, Muñoz-Torrico M, Salazar-Lezama MA, Selman M, Fallert-Junecko B, Reinhardt TA, Alcorn JF, Kaushal D, Zuñiga J, Rangel-Moreno J, Kolls JK, Khader SA. 2017. Novel role for IL-22 in protection during chronic Mycobacterium tuberculosis HN878 infection. Mucosal Immunol 10:1069–1081. https://doi.org/10.1038/mi.2017.15.
21. Nagy C, Haschemi A. 2015. Time and demand are two critical dimensions of immunometabolism: the process of macrophage activation and the pentose phosphate pathway. Front Immunol 6:164. https://doi.org/10.3389/fimmu.2015.00164.
22. Baardman J, Verberk SGS, Prange KHM, van Weeghel M, van der Velden S, Ryan DG, Wüst RCI, Neele AE, Speijer D, Denis SW, Witte ME, Houtkooper RH, O'Neill LA, Knatko EV, Dinkova-Kostova AT, Lutgens E, de Winther MPJ, Van den Bossche J. 2018. A defective pentose phosphate pathway reduces inflammatory macrophage responses during hypercholesterolemia. Cell Rep 25:2044–2052.e5. https://doi.org/10.1016/j.celrep.2018.10.092.
23. Tannahill GM, Curtis AM, Adamik J, Palsson-McDermott EM, McGettrick AF, Goel G, Frezza C, Bernard NJ, Kelly B, Foley NH, Zheng L, Gardet A, Tong Z, Jany SS, Corr SC, Haneklaus M, Caffrey BE, Pierce K, Walmsley S, Beasley FC, Cummins E, Nizet V, Whyte M, Taylor CT, Lin H, Masters SL, Gottlieb E, Kelly VP, Clish C, Auron PE, Xavier RJ, O'Neill L. 2013. Succinate is an inflammatory signal that induces IL-1β through HIF-1α. Nature 496:238–242. https://doi.org/10.1038/nature11986.
24. Lampropoulou V, Sergushichev A, Bambouskova M, Nair S, Vincent EE, Loginicheva E, Cervantes-Barragan L, Ma X, Huang S-C, Griss T, Weinheimer CJ, Khader S, Randolph GJ, Pearce EJ, Jones RG, Diwan A, Diamond MS, Artyomov MN. 2016. Itaconate links inhibition of succinate dehydrogenase with macrophage metabolic remodeling and regulation of inflammation. Cell Metab 24:158–166. https://doi.org/10.1016/j.cmet.2016.06.004.
25. Puleston D. 2015. Detection of mitochondrial mass, damage, and reactive oxygen species by flow cytometry. Cold Spring Harb Protoc 2015:pdb.prot086298. https://doi.org/10.1101/pdb.prot086298.
26. Crowley LC, Christensen ME, Waterhouse NJ. 2016. Measuring mitochondrial transmembrane potential by TMRE staining. Cold Spring Harb Protoc 2016:pdb.prot087361. https://doi.org/10.1101/pdb.prot087361.

Downloaded from https://journals.asm.org/journal/iai on 06 February 2025 by 18.97.14.90.